Detecting the Zero-Crossing Message to Achieve Low Bit Transmission over H-bridge Inverter

A. R. Ndjiongue, A. J. Han Vinck‡, K. Ouahada, H. C. Ferreira and A. J. Snyders
Department of Electrical and Electronic Engineering Science, University of Johannesburg,
P.O. Box 524, Auckland Park, 2006, Johannesburg, South Africa.
‡Institute of Experimental Mathematics, University of Duisburg-Essen,
Ellernstr. 29, 45326 Essen, Germany.
Email: {alainn, kouahada, hcferreira, ajsnyders}@uj.ac.za, vinck@iem.uni-due.de

***Abstract*—Home automation and smart grid development is motivated by many advantageous situations that include the demands on renewable energy and the advantages provided by power line communications technology (PLC). The integration of solar energy into conventional grid implies the control of different modules included in the system. Remote control seems to be the control mode by excellence, in which communication is the main point to focus on. The pulse width modulation (PWM) scheme used to control the inverter is also used to modulate the zero-crossing point of the output sine wave of the inverter, to transfer data. The zero-crossing modulation technique is proposed and basic elements to construct the model are proposed. Simulated constellations of the received signal are presented.**

Keyword: PLC, zero-crossing, modulation, PWM control, AWGN, phase noise and Jitter

I. Introduction, motivation

The growing demand in the renewable energy area is motivated by the ratification of the convention on Greenhouse gas emissions. Among the available solutions, green energies represent the option that can also be used for the electrical energy consumption reduction. Integrating renewable energies into the conventional grid enable a new topology of the electrical network. That new topology allows 2 ways flow of energy, from the utility to the end consumer and vice versa. Zigbee is the leading technology in grid connected systems [1]. Actually Zigbee permits an excellent grid tied control and monitoring. Unfortunately it presents some defects, especially when it is to deal with basements of tall buildings, as well, when the signal has to pass through thick walls. The carrier signal is blocked and the remote control of the system is impossible. The solution is to use wire based technologies, but for cost purpose, it will not be accepted to run additional wires between modules. Power line communications (PLC) technology is then appealed. It uses the power wire to transport data. One of the main challenges while trying to use PLC in solar energy is the power electronic modules [inverter and booster] inserted between the solar panel and the load (grid). For the frequencies between 3 kHz and 500 kHz, the noise level is very high inside the inverter. This is due to the presence of the predominant low frequency noise components. Fig. 1 extracted from [2] shows the spectrum of the noise inside the inverter. The low pass output filter attenuates all high frequency signals in the inverter; but lower frequencies are welcome. Also, the noise

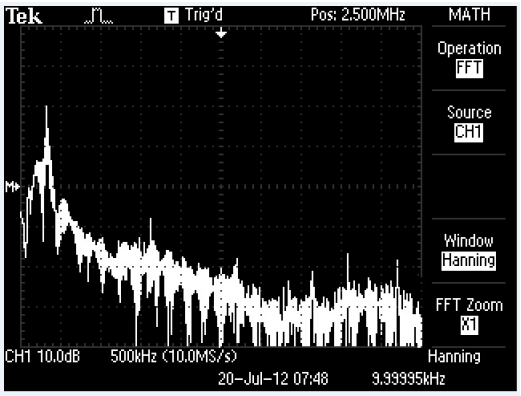

Fig. 1. Inverter noise spectrum

level decreases considerably the signal to noise rate (SNR) to a very low value. Therefore, Zero-crossing technique seems to be the scheme solution. Zero-crossing modulation is the purpose of this paper. The modulator is the control unit of the inverter. The detection is the process of identifying the presence of the message concealed by the sender as mentioned in [2]. The detection of the time difference referenced to a sampling time of the original zero-crossing, misted to additive noise (AWGN), to phase noise, and to jitter deviation seems to be the challenge. The system incorporates many blocks. The rest of the paper is organized as follows: The impact of the zero-crossing change on the system is highlighted in Section II. The inverter design concept is presented in Section III, followed by the proposed zero-crossing detection principle in Section IV. Section V defines the bandwidth of the communication system while Section VI analyses the transmission system when the communication is corrupted by AWGN or phase noise and jitter. The simulation setup is given in Section VII. The paper is concluded in Section VIII.

II. Inverter design and impact of the zero changing

In the case of this study, the output of the inverter is a pure sine wave. The chosen topology is H-Bridge. This topology is indicated for renewable energy [3]. The model proposed in

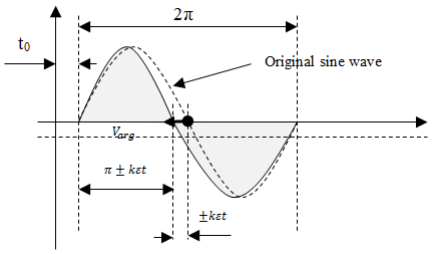

Fig. 2. Illustration of the zero-crossing highlighting the average voltage

[4] motivates the choice of the number of switches (4) and the number of phases (1).

Any change on the output of the inverter, on the DC bus, as well as the variation of the solar panel output will affect the PWMs. The control unit uses these changes to monitor the system. The drivers are assigned to connect the PWM outputs to the gate of the switches (Insulated-gate bipolar transistors (IGBTs) in this case).

The power stage is made of 4 switches. They are closed and opened two by two. Each pair receives an input gate signal from a gate driver. One IGBT receives the signal from the high-side driver output while the other one receives the signal from the low-side driver output causing one to be on and the other to be off during one half-cycle [5-6]. They then change states for the other half cycle. The other pair of IGBTs will be driven by a gate driver with a 50 Hz square wave input. The output signal will be a zero centered. An output low pass filter will help producing a pure sine wave.

A. Impacts of the zero-crossing changing

The effective value of the output signal is given by (1). It is not different from the one of the pure sine wave presented in (2).

$$V_{rms}^2 = \frac{1}{T}[\int_0^{\frac{T}{2}\pm k\varepsilon t} v(t)^2 dt + \int_{\frac{T}{2}\pm k\varepsilon t}^{T} v(t)^2 dt] \quad (1)$$

$$V_{rms}^2 = \frac{1}{T}[\int_0^{T} v(t)^2 dt] \quad (2)$$

When the zero-crossing point moves, the average voltage is not null. In (3), the expression of the average voltage of the modulated signal is given:

$$V_{avg} = \frac{2}{T}[\int_0^{\frac{T}{2}\pm k\varepsilon t} v(t)dt] - \frac{2}{T}[\int_{\frac{T}{2}\pm k\varepsilon t}^{0} v(t)dt] \neq 0, \forall k \neq 0 \quad (3)$$

Fig. 2 illustrates the presence of a DC component in the output voltage when the zero-crossing point changes its position.

III. Zero-crossing detection principle

The sampling process is used to detect the message. The sine wave is a power signal from the solar system powering the load. Its mathematical expression is given by:

$$v(t) = V_m e^{j(2\pi f_a t + \varphi_v)} \quad (4)$$

and the Dirac function is given by:

$$\int_{-\varepsilon}^{+\varepsilon} \delta(t)dt] = 1 \quad (5)$$

The following equation traces a possible combination between (4) and (5), which is an important property of the Dirac function.

$$\int_{-\infty}^{+\infty} v(t).\delta(t)dt = v(t) \quad (6)$$

$\delta(t)$ multiplies $v(t)$; only the instant where the product $v(t) \times \delta(t)$ is null is considered. That instant points on the zero crossing point of $v(t)$. The product $v(t) \times \delta(t)$ is null when (7) is satisfied.

$$\int_{-\infty}^{+\infty} V_m e^{j(2\pi f_a t + \varphi_v)}.\delta(t)dt = 1 \quad (7)$$

The principle of detection is based on converting the time difference εt between the original crossing point and the new crossing time. Let t_c be the new crossing time, t_0 the original crossing time, the detector calculates the time difference $\varepsilon t = t_0 \pm t_c$ and converts it into angle (see (8)). The detector scans one cycle of the sine wave and saves each time the result in a memory. The scanning consists of producing at the clock frequency a Dirac impulse, multiplied by the voltage each time during the period of the sine wave. The scanning done, the time difference εt is converted into angle and the result is communicated to the demodulator. Practically, the conversion is to calculate the angle for each position of the zero. The phase fluctuation $\theta(t)$ is then related to the time fluctuation $\tau(t)$ by the following equation:

$$\theta(t) = 2\pi f_0 \tau(t) \quad (8)$$

The variations $0, \varepsilon t_0, 2\varepsilon t_0 \ldots k\varepsilon t_0$ are converted into angle (see (8)) and into binary to recover the message. The provoked phase error will create unbalance on the sine wave, resulting on a non-ideal periodic sine wave function. At $t_c = \pi \pm k\varepsilon t, \int v(t) \times \delta(t) = 1$. (9) converts t_c into angle.

$$k(t_c - t_0) = \pm k\varepsilon t = \frac{\pm k\varepsilon\theta}{2\pi f_a} \quad (9)$$

On Fig. 3, Ω and Ω' are assumed to be parallel in the fraction of time $k\varepsilon t$. The reason is that $k\varepsilon t$ is very small and closed to 0, but not null. According to the assumption made above, we can express the time variation of the zero-crossing using the voltage variation as,

$$\varepsilon t = \frac{\varepsilon v}{2\pi f_a V_m}, \quad (10)$$

and the variation of the angle is then rewritten as,

$$\varepsilon\theta = \frac{\varepsilon v}{V_m}. \quad (11)$$

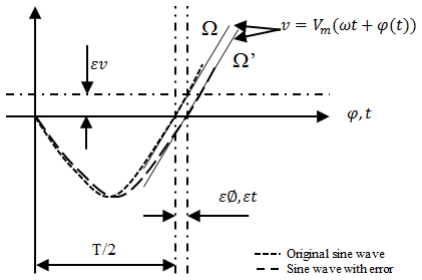

Fig. 3. Illustration of a positive zero-crossing, showing the phase and time error

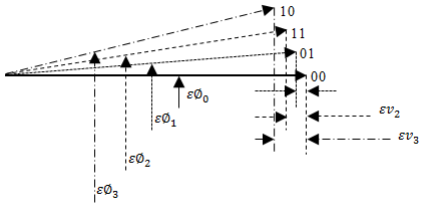

Fig. 4. Constellation of the zero-crossing considering 4 symbols

The error voltage (εv) due to the zero-crossing changing expressed in (11) will define the SNR of the transmission. Jitter and phase disturbances have been intensively studied in [7]. The authors expressed the maximum error derived from the total noise and the provoked deviation of the crossing point by $\varepsilon v_m = \varepsilon t V_m 2\pi f_a$, then the angle variation can be expressed as $\varepsilon\theta = \varepsilon t 2\pi f_a$. For the maximum acceptable distortion on the sine wave, the quantity $\varepsilon t V_m 2\pi f_a$ must be very little, less than 10% of V_m, which corresponds to a total deviation of $\frac{\pi}{32}$.

For four different errors introduced in the system, we can detect four different symbols. The constellation for four angles errors is illustrated on Fig. 4. The symbols will be mapped to the four complex numbers $0 + j0$, $0.99 + j0.07$, $0.98 + j0.15$, $0.97 + j0.23$, and $0.95 + j0.31$. In case of two symbols, the mapping is going to be done between $0.99 + j0.07$ and $0.95 + j0.31$, which will be more accurate in terms of SNR. Changing the specifications (RLC) of the load, will drastically affect the sine wave and the state of the bits sent can jump from one binary value to another.

IV. Zero-crossing bandwidth

For the amount of data that can be transmitted in a second, we look at the total possible deviation of the zero crossing. To proceed, we analyse (11) and extract the expression of εv to determine the maximum amount of DC component that will less distort the sine wave. The quantity εv and the DC component in the signal are linearly correlated. Since the frequency at the inverter output is 50 Hz, the wave length duration is 0.02 s. In 1 s we have 50 alternations. 32 alternations will be used to transport 2 bits each, which represent 64 bits per second, this amount can significantly be increased if the load is not a critical load. Assuming that the deviation of the zero crossing point will start to distort the sine wave at $\varepsilon v = 10\ \%$ of the maximum value; then the maximum deviation allowable is εt_m=1 ms. This corresponds to a deviation $\varepsilon t_{m/s}$=0.02 ms per symbol. Each symbol representing a strings of 2 "0" or "1", then a bit length of 10 μs is allowed. the value $\varepsilon v = 0.001 \times 220\sqrt{2} \times 2\pi = 1.955V$, corresponding to a deviation εt_m=1 ms is negligible compared to the maximum value of the voltage ($311V$). More we increase the deviation, more the bit rate increases, then the bandwidth can be expressed as a function of the the deviation of the crossing point by the relation in (12). The demodulation is based on the principle of phase shift keying (PSK). But only on the first quarter of the constellation plan. The principle of high order PSK scheme has being largely developed in the literature [8-11].

$$B = B_m \frac{\varepsilon t}{\varepsilon t_m} \tag{12}$$

where B is the bandwidth in Bps, B_m is the maximum bandwidth allowable, εt is the deviation and εt_m is the maximum deviation allowable to keep the system stable. The bandwidth is also given by the relation $B = B_m \varepsilon t 2^N / V_m$, ($\varepsilon t_m = V_m / 2^N$) [7], where N represents the number of bits sent. The bandwidth can then be rewritten as:

$$B = B_m \frac{(\varepsilon t)^2 2^N 2\pi f_a}{\varepsilon v_m} \tag{13}$$

(13) can be reduced to $B = 400\pi B_m \frac{(\varepsilon t)^2}{\varepsilon v_m}$ (with f_a=50 Hz and $N = 2$).

V. In presence of noise

A. Additive noise (AWGN)

The signal vector is given by,

$$s(t) = Se^{(2\pi f_a t + \varphi_s)} \tag{14}$$

$s(t)$ is derived from the 220 V_{RMS}, $r(t)$ is obtained at the output of the system when the noise corrupts the signal. Let $h(t)$ be the matched filter transfer function optimised using the correlation receiver principle. Adding the noise, the output of the channel presents the following vector, including the transmission delay t_0.

$$r(t) = s(t - t_0) + w(t) \tag{15}$$

The accuracy of the receiver will present the possible highest definition when the signal to noise ratio (SNR) will be the maximum. A simple way of adjusting the SNR is the insertion in the system of a matched filter. $r(t)$ is presented at the filter input and convoluted by $h(t)$. The output of the filter is defined by $m(t)$ as

$$m(t) = x(t) * h(t). \tag{16}$$

The filter output can be rewritten using the input signal, including the transmission delay t_0 as,

$$m(t) = s(t - t_0) * h(t) + w(t) * h(t). \quad (17)$$

The matched filter filters both signal and noise. The quantity $s(t - t_0) * h(t)$ represents the received filtered signal while $w(t)*h(t)$ represents the filtered noise component. To optimise the SNR, the filter must maximise the quantity $s(t-t_0)*h(t)$ and minimise $w(t) * h(t)$. To do this, the filter realises the expression of the SNR given in (18), assuming the noise been AWGN.

$$SNR = \frac{[s(t - t_0) * h(t)]^2}{E[w(t) * h(t)]^2} \quad (18)$$

Given the fact that AWGN variance is defined by $\sigma^2 = \frac{N_0}{2}$, the SNR can be rewritten as,

$$SNR = \frac{[\int_{t_0}^{t_0+t} s(\omega)h(t-\omega)d\omega]^2}{\frac{N_0}{2}\int_{t_0}^{t_0+t} h^2(t-\omega)d\omega}. \quad (19)$$

After applying the inequality of Cauchy-Schwartz, (19) leads to,

$$SNR = \frac{[\int_0^t s^2(\omega)d\omega]}{\frac{N_0}{2}}, \quad (20)$$

where $s(t)$ has finite duration T and SNR is maximized during one wave length T. We assume the following equality: $T/2 \pm \varepsilon kt \approx T/2$, then the optimum SNR can be expressed by,

$$SNR \approx \frac{2\varepsilon_s}{N_0} \quad (21)$$

(where ε_s is the energy of the sent signal)

B. Impact of the phase noise and jitter

Amplitude noise, phase noise and Jitter as any other noise, cause error in all communication systems. Phase noise and jitter are the cause of the horizontal fluctuation of the transition timing across the crossing point for a given signal, while amplitude noise expands the amplitude of a given signal. A sample clock can be considered as a periodic square wave with rising and falling edges representing at a fixed time interval Γ such that $\Gamma = 1/f_s$, f_s being the sampling frequency; jitter is defined as an additive time variation Δt; added to the fixed period Γ, the resulting period is giving by the relation $\Gamma = 1/f_s \pm \Delta t$, see Fig. 5. Similarly, phase noise is defined as an arbitrary function $\alpha(t)$ such that a sinusoidal function can be written as a function of t and $\alpha(t)$. In [12], a signal with jitter noise is defined as a double function of t in time domain. See (22), where $j(t)$ represents the jitter noise disturbance of the time variable in seconds, $r_j(t)$ is the received signal affected by the jitter disturbance.

$$r_j(t) = R_j sin[2\pi f_a(t + j(t)) + \varphi_s] \quad (22)$$

If the sent signal $s(t)$ is affected by a phase noise and an amplitude noise, an arbitrary function $\alpha(t)$ is inserted to $s(t)$ and the received signal is given in (23). The final noisy function includes the amplitude noise (AM) $\beta(t)$, and $\alpha(t)$ is the phase modulation noise (PM).

$$r_p(t) = R_p[1 + \beta(t)]sin(2\pi f_a t + \varphi_s + \alpha(t)) \quad (23)$$

It is shown that amplitude noise can be misinterpreted for phase noise since both forms of noise cause similar faults and errors on the received message. Frequency noise and phase noise are shown to be closely related to each other. All these perturbations affect the bit error rate [13]. The impact of the amplitude noise in this study is assumed to be negligible because of the modulation scheme in application therefore, $\beta(t) = 0$; then the final expression of $r_p(t)$ is given as,

$$r_p(t) = R_p sin(2\pi f_a t + \varphi_s + \alpha(t)). \quad (24)$$

Phase noise is frequency dependent and according to [14], becomes white around 10^8 Hz, but that threshold is related to the specifications of the components used in the circuits. In [13], the authors simulated the phase noise and the result gives an asymptotic phase course indicating that the phase noise becomes white around 10^3 Hz. In [13] and [14], it is shown that phase noise is more important at low frequency.
The system includes the inverter control cadenced at high frequency to reduce the flickering and to minimize the jitter effects. But It is still to be used a jitter compensator block and a synchronizer block to reduce the impact of undesired deviations. It is presented in [15] that the timing error variance is given using some assumptions; the zero-crossing point is sufficiently close to the nominal crossing point, so that two terms Taylor series expansion can be used. Then, considering a system with additive noise in this case, the zero-crossing position in the received signal will occur at t as,

$$t = \frac{kT}{2} \pm k\varepsilon t + t_0 \pm (w_k + \tau_k + \varepsilon_k) \quad (25)$$

where t_0 is the transmission delay, $kT/2 \pm k\varepsilon t$ represents the provoked deviation, w_k is a parameter due to the additive noise, τ_k is due to the symbol overlap and ε_k is due to the jitter and the phase noise. But, since there is no overlap, $\tau_k = 0$. The synchronizer is built based on the time t computed in (26). At low frequency of the signal, the system is not impacted by jitter noise [7], ε_k is then due only to the phase noise.

$$t = \frac{kT}{2} \pm k\varepsilon t + t_0 \pm (w_k + \varepsilon_k) \quad (26)$$

Looking at Fig. 5, the expected crossing point occurs at $T/2 + \varepsilon t$, the real zero-crossing occurs at $T/2 + \varepsilon t \pm \Delta t$; Δt is due to the total noise. Comparing the SNR in presence of the total noise to the one calculated in presence of the AWGN alone, the SNR will decrease for low sampling frequencies. For high frequencies sampling, jitter noise combine to phase noise becomes white and the SNR is closed to the one calculated for a system corrupted by AWGN . Taking into account the total noise, N_0' represents the power spectral density of the sum of the disturbances.

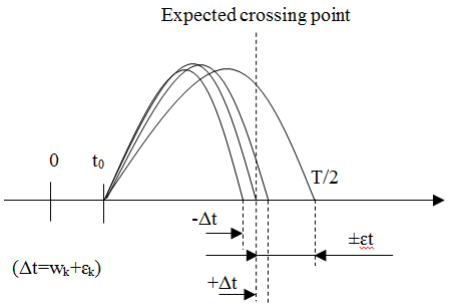

Fig. 5. Illustration of the real crossing point in presence of phase noise, jitter and AWGN

$$SNR = \frac{2\varepsilon_s}{N_0'} \tag{27}$$

According to the fact that the transmission does not inject any signal into the channel, it is very useful to express the SNR as a function of the derivation error observed on the received signal. As presented in Fig. 5, the time error due to phase noise and additive noise is expressed as $\Delta t = w_k + \varepsilon_k$, this can be converted into angle ($\Delta\theta$). Considering the expression of the voltage $v(\theta) = V_m sin\theta$, the slope of $v(\theta)$ at the deviation point is given by $v'(\theta) = dv/d\theta$. Let $\varepsilon v(\theta)$ be the error voltage due to the total sum of noise, $\varepsilon v(\theta)$ is defined as,

$$\varepsilon v(\theta) = v'(\theta) d\theta. \tag{28}$$

The mean square of $\varepsilon v(\theta)$ is given by:

$$E[\varepsilon v(\theta)^2] = E[v'(\theta)^2 d\theta^2] \tag{29}$$

Then, the signal to noise ratio SNR can be expressed as

$$SNR = \frac{E[v(\theta)^2]}{E[\varepsilon v(\theta)^2]}. \tag{30}$$

Knowing the signal power $E[v(\theta)^2] = V_m/2$, and the error power $E[\varepsilon v(\theta)^2] = \Delta\theta^2 V_m/2$ with $\Delta\theta^2$ being the variance of the total noise expressed as a function of the angle variation (θ) [7], the SNR is then re-written as,

$$SNR = \frac{1}{\Delta\theta^2} \tag{31}$$

In decibel, the signal to noise ratio can be expressed as given in (32) as:

$$SNR = -20log_{10}[\Delta t 2\pi f_a] \tag{32}$$

VI. Bit error rate estimation and simulation setup

In systems having low rates of E_b/N_0, the final AWGN and phase noise (PN) BER is predominantly affected by the presence of AWGN. While in systems with high rates of E_b/N_0, the final AWGN and PN BER is determined by taking into consideration the presence of PN. The final AWGN and PN BER course is asymptotically nearing to the individual PN-BER course [13].

Signal to noise ratios and E_b/N_0 figures are parameters that are more associated with radio connectivity and radio communications systems. To determine the BER , three important parameters are to be defined: the error function *erf*, the energy in one bit, E_b, and the noise spectral density N_0 , representing the noise power in a 1 Hz bandwidth. The energy per bit E_b can be determined by dividing the carrier power by the bit rate. The interference present in the system is generally set by external factors and cannot be changed by the system design. Though, it is possible to set the bandwidth of the system. Reducing the bandwidth will reduce the interference but will limit the throughput that can be achieved.

A. Simulation setup

In [16], the authors analysed a system with phase noise. Their paper gives a model of phase noise with a variance given by $\sigma^2 = 2\pi\beta T/N$, where T represent the symbol length, β is the phase linewidth and N the number of data symbols. With analogy, the above mentioned variance will be used in the simulation to represent the phase noise disturbance. In [17], the authors presented the common error due to phase shift and phase noise. They presented the discrete phase noise in a receiver as a function of the number of symbols by $\Phi(i+1) = \Phi(i) + w(i)$ where the $w(i)$ is a Gaussian random variable with zero mean and its variance σ_w is given by $\sigma_w^2 = 4\pi^2 f_c^2 c T_s$. The total noise affecting the transmission is represented by its variance (σ_n), with $\sigma_n^2 = \sigma_w^2 + \sigma_\varepsilon^2$ (where ω and ε where defined (26)). The total noise variance is given by,

$$\sigma_t^2 = 4\pi^2 f_c^2 C T_s + 2\pi\beta\frac{T}{N} \tag{33}$$

where T_s is the sampling period adjusted to the control frequency of the inverter, f_c is the carrier frequency, $50Hz$ in this case, and C is the discretized Brownian motion process [18].

B. Constellations

Fig. 6 represents four different constellations for 4.5^o provoked deviation. The message length starts to be noticeable from 35 dB SNR. Figures 7 and 8 are respectively the constellations for 18^o and 30^o, for four different values of the signal to noise rate. Since we used an angular representation, when the angle increases, the tau of error decreases and the reception becomes more accurate.

VII. Conclusion

In this paper, the zero crossing modulation of the sine wave for smart grid purpose was proposed and presented. The principle of detection was presented. The detection is based on the time difference between the original zero and the new crossing point. The impact of the zero-crossing modulation on the load depends on the quantity $\varepsilon\theta = \varepsilon v/V_m$. The maximum bandwidth B_m depends on the maximum possible deviation Δt_m occurring on the received sine wave. For this

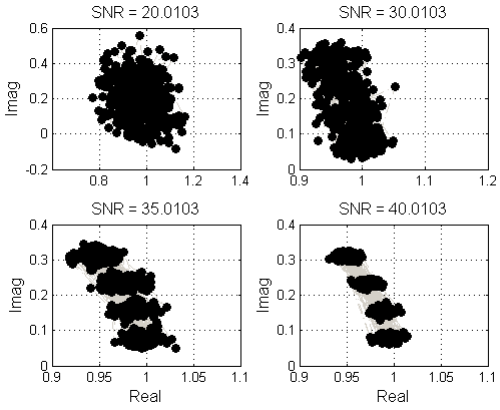

Fig. 6. Constellation for Zero-C for 4.5^o

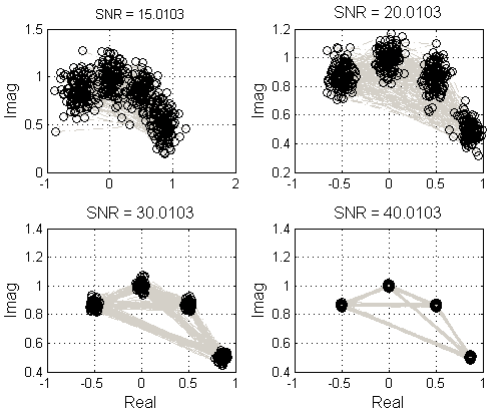

Fig. 8. Constellation for Zero-C for 30^o

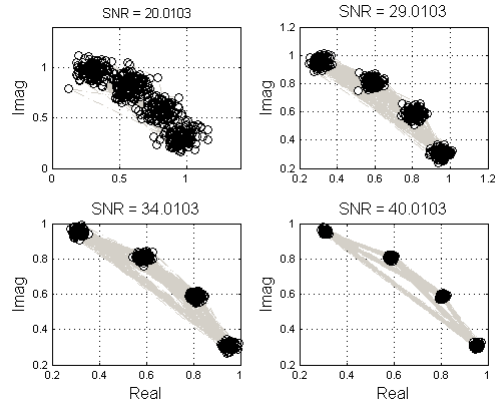

Fig. 7. Constellation for Zero-C for 18^o

transmission to perform better, the accuracy of the inverter control, source of the message, is the most critical part to focus on. For critical loads, the voltage error due to the transmission must not be greater than the tenth of the voltage, otherwise the load need to be resistive.

REFERENCES

[1] F.Richard, Yu, P. Zhang, W. Xiao, and P. Choudhury, Communication System for Grid Integration of Renewable Energy Resources. IEEE Network, vol. 25, pp. 22 29, Sept./Oct. 2011.

[2] A. R. Ndjiongue, A. J. Snyders, H. C. Ferreira and M. Della Tamin, "H-Bridge Inverter as Part of the Communication Channel for Deploying Power Line Communications Over Solar Photovoltaic Energy System", 17^{th} IEEE International Symposium on Power Line Communications and Its Applications (ISPLC), pp. 114-119, 24-27 March 2013, Johannesburg, South Africa.

[3] S. Jain, V. Agarwal "A Single-Stage Grid Connected Inverter Topology for Solar PV Systems with Maximum Power Point Tracking", IEEE transactions on power electronics, vol. 22, n^o. 5, September 2007

[4] M. Sasikumar, S. C. Pandian, "Modeling and Analysis of Cascaded H-Bridge Inverter for Wind Driven Isolated Self Excited Induction Generators" International Journal on Electrical Engineering and Informatics Vol. 3, n^o 2, 2011

[5] A. Nabae, I. Takahashi and H. Akagi, "A New Neutral-Point-Clamped PWM Inverter". IEEE Transaction on Industry Applications, vol. IA 17, n^o. 5, pp. 518 523, Sept. 1981

[6] Krismadinata, N. A. Rahim, and J. Selvaraj, "Implementation of Hysteresis Current Control for Single-Phase Grid Connected Inverter". 7^{th} International Conference on Power Electronics and Drive Systems ($PEDS$07), pp. 1097 1101, 27 30 Nov. 2007

[7] Carlos Azeredo-Leme, "Clock Jitter Effects on Sampling: A Tutorial" IEEE Circuit and System Magazine, vol. 11, n^o. 3, pp. 26-37, 22 Aug. 2011

[8] J. Lee, S. Cho, "A Low Power Transmitter for Phase-shift Keying Modulation Schemes", 17^{th} IEEE International Symposium on Personal Indoor and Mobile Radio Communication, pp. 1-5, 11-14 Sept. 2006

[9] G.. C. Cardarilli, A. Del Re, M. Re, L. Simone, "Optimized QPSK modulator for DVB-S applications" IEEE International Symposium on Circuits and Systems, ISCAS 2006, 21-24 May 2006

[10] S. Z. Ibrahim, A. M. Abbosh, M. A. Antoniades, "Direct quadrature phase shift keying modulation using compact wideband six-port networks" IEEE Journals and Magazines on Microwaves, Antennas and propagation IET, vol. 6, n^o. 8, pp. 854-861, June 7 2012

[11] M. L. Boucheret, I. Mortensen, H. Favaro, E. Belis, "A new algorithm for non-linear estimation of PSK-modulated carrier phase", 3^{rd} European conference on Satellite Communications $ECSC$-3, pp. 155-159, 2-4 Nov. 1993

[12] Un-Ku Moon, K. Mayaram, J. T. Stonick, "Spectral Analysis of Time-Domain Phase Jitter Measurements", IEEE transactions on circuits and systems-II: Analogue and Digital Signal Processing, vol. 49, n^o. 5, May 2002.

[13] O. Baran, M. Kasal, P. Vagner and T. Urbanec, "Phase Noise Impact on BER in Space Communication" World Academy of Science, Engineering and Technology 69, 2012.

[14] T. Wen, T. Kwasniewski, "Phase Noise Simulation and Modeling of ADPLL by SystemVerilog", IEEE International Workshop on Behavioral Modeling and Simulation , pp. 29-34, 25-26 Sept. 2008. Jan Jose, Canada.

[15] P. G. Ogmundson, P. F. Driessen, "Zero-Crossing DPLL Bit Synchronizer with Pattern Jitter Compensation" IEEE Transactions on Communications, vol. 39, n^o. 4, April 1991

[16] M. Mahbubur Rahamn, Md. Delowar Hossain, ABM Shawkat Ali, "Performance Analysis of OFDM Systems with Phase Noise" 6^{th} International Conference on Computer and Information Science IEEE/ACIS, pp.358-362, 11-13 July 2007, Melbourne, Australia.

[17] D. petrovic, Wolfgang Rave and Gerhard Fettweis, "COMMON PHASE ERROR DUE TO PHASE NOISE IN OFDM-ESTIMATION AND SUPPRESSION", 15^{th} International Symposium on Personal, Indoor and Mobile Radio Communication, IEEE/PIMRC, vol. 3, pp. 1901-1905, 5-8 Sept. 2004

[18] A. Demir, A. Mehrotra, J. Roychowdhury, "Phase noise in oscillators: a unifying theory and numerical methods for characterization", IEEE Transactions on Circuits and Systems I: Fundamental Theory and Applications, vol. 47, n^o. 5, pp. 655-674, 06 August 2002.